PNAS
www.pnas.org

Supplementary Information for

Increasing valence pushes DNA nanostar networks to the isostatic point

Nathaniel Conrad, Tynan Kennedy, Deborah K. Fygenson, and Omar A. Saleh

Nathaniel Conrad.
E-mail: nconrad@ucsb.edu

This PDF file includes:

www.pnas.org/cgi/doi/10.1073/pnas.1819683116

Supporting Information Text

S1. DNAns-specific information

This section includes information regarding the DNA sequences used for each DNA Nanostars (DNAns) design, DNA concentration measurements, binding probability calculations, and hysteresis of structure formation:

S1a. DNA sequences. Each of the f single-stranded (ss) DNA segments required to make $f = 3, 4, 5$, and 6 DNAns are 49 nucleotides long. In each sequence, 40 of the nucleotides are designed to form portions of an arm, 6 constitute the sticky-end, and 3 are unbound (Fig. S1).

S1b. Binding probability and mean valence calculations. We can get a sense of the magntiude of the change in connectivity from calculating the binding probability, p_b, between two DNAns arms. p_b was calculated in a mean-field approximation that ignores connectivity using the DNA thermodynamics package NUPACK (1). For our overhang sequence 5′-ACGTACG-3′, and an oligo concentration of f·[DNAns], we find that $p_b > 0.84$ at $T = 35°C$, the highest temperature explored, and grows slowly to $p_b \approx 1$ at $T = 5°C$ (see Fig. S2). This leads to a predicted mean-valence, $\langle z \rangle \approx p_b f \approx 0.98 f$ at $T_{\rm ref} = 20°C$. The use of such a model to calculate p_b for the DNA nanostar system was quantitatively validated by Rovigatti *et. al.* (2) in comparison to DNAns simulations that incorporate connectivity.

S1c. Concentration measurements. We used a droplet spectrophotometer (Nanodrop 2000c; Fisher Scientific) to measure the absorption at 260 nm (A260) and derive the DNAns concentration, [DNAns], of f-armed DNAns solutions (Fig. S3 and Fig. S4). The A260 of an f-armed DNAns solution is related to its [DNAns] by

$$[\text{DNAns}] = \text{A260}/(\Sigma_i \epsilon_i) \qquad [1]$$

where ϵ_i is the extinction coefficient of the $i^{\rm th}$ ss DNA segment composing the f-armed DNAns (see Fig. S1 for the extinction coefficients). Note that equation 1 assumes all DNAns in solution have completely denatured into their single stranded components.

The DNAns concentrations of solutions prepared for the rheometer were so large that their A260 could not be measured directly. The A260 of solutions diluted 100-fold, $\text{A260}_{1\%}$, in pure water was measurable, but we questioned whether this dilution was sufficient to completely denature the DNAns and permit the use of equation 1. To check, we compared the A260 of a 100-fold dilution of the most concentrated sample of a given valence, $\text{A260}^*_{1\%}$, to the A260 of a 10,000-fold dilution made in pure water from that same 100-fold dilution, $\text{A260}^*_{0.01\%}$. In all cases, $100{\cdot}\text{A260}^*_{0.01\%} \geq \text{A260}^*_{1\%}$, consistent with incomplete denaturation at 100-fold dilution (Table S1).

The proportion of single-stranded DNA present in the 100-fold diluted solutions, α, can be calculated based on the extinction coefficients of single-stranded (ss) and double-stranded (ds) DNA (3)

$$\epsilon_{\rm ss} = [37\,\mu\text{g}/(\text{mL}\cdot\text{cm})]^{-1} \qquad \text{and} \qquad \epsilon_{\rm ds} = [50\,\mu\text{g}/(\text{mL}\cdot\text{cm})]^{-1}$$

given that the absorbance of the 1% solution is due to both ss and ds DNA

$$\text{A260}^*_{1\%} = \alpha\,\frac{c}{37} + (1-\alpha)\,\frac{c}{50} \qquad [2]$$

and assuming the absorbance of the 0.01% solution is due to only ss DNA

$$\text{A260}^*_{0.01\%} = 0.01\,\frac{c}{37}\,, \qquad [3]$$

where c is the total mass concentration of DNA present in the 1% solution. Dividing equation 2 by 3, we can derive an expression for α:

$$\alpha = \left(\frac{\text{A260}^*_{1\%}}{\text{A260}^*_{0.01\%}} - 74\right)/26 \qquad [4]$$

We found α ranged from $\approx 30\%$ for the most concentrated 3-arm nanostar solutions, to $\approx 96\%$ for the most concentrated 6-arm nanostar solutions (Table S1). We note that we assumed α was concentration independent and only measured the α of the most concentrated solution at a given f in order to interpret the $\mathrm{A260}_{1\%}$ of all (less concentrated) solutions of a given f-armed nanostar and, thus, avoid an excessive amount of multi-step dilutions.

Since α tracks the correct portion of ss and ds DNA present at the 1% dilutions, we used it to correct the measured [DNAns] from the respective $\mathrm{A260}_{1\%}$ measurement because using equation 1 assumes the 1% solution contains only ss DNA (*i.e.*, equation 1 assumes $\mathrm{A260}_{1\%} = c/37$). The correction is found by dividing the ideal A260 for ss DNA solutions, $\mathrm{A260}_{\mathrm{ss}} = c/37$, by equation 1:

$$\text{correction} = \mathrm{A260}_{\mathrm{ss}}/\mathrm{A260}^{*}_{1\%} = 1/(0.24 \cdot \alpha + 0.76) \qquad [5]$$

For the lowest and highest measured α, the correction to the concentration was $\approx 23\%$ and $\approx 1\%$, respectively (Table S1). We note that the error introduced to the [DNAns] by assuming a concentration-independent α has little to no effect ($<< 1\%$ error) on the scaling exponents measured from the $G'_p([\mathrm{DNAns}])$ data because the relative ratio of concentrations are kept the same when using a concentration-independent correction.

S1d. Hysteresis measurements. We tested for hysteresis of structure formation by repeatedly measuring the storage, G', and loss, G'', modulus as a function of temperature at $\gamma = 5\%$, $\omega = 10$ rad/s, and at two different rates of temperature change, $|dT/dt| = 1.5$ and 15°C/min. G' and G'' were independent of the rate of cooling and heating for rates $|dT/dt| \leq 15$°C/min for all f and [DNAns] (Fig. S5). The rate at which temperature changed between the different temperature measurements of $G'(\omega, T)$ and $G''(\omega, T)$ contributing to the master curve was $|dT/dt| \leq 15$°C/min. Thus, all DNAns networks studied here form reversibly and are always in equilibrium.

S2. Frequency sweep technical information

This section includes information regarding time-temperature superposition (i.e., master curve construction) and network relaxation time:

S2a. Time-temperature superposition. Time-temperature superposition (TTS) constructs a material's viscoelastic response over a wide range of frequencies by superimposing frequency sweeps made at different temperatures onto one another. The resulting superimposed curve is known as the "master curve". We used the TTS protocol provided in the rheometer's proprietary software (TRIOS v.4.0.1, TA Instruments) to construct master curves at a reference temperature of $T_{\mathrm{ref}} = 20°C$, allowing for both vertical and horizontal shifts of the raw frequency sweeps. An example of the TTS process is illustrated in Figure S6. Figures S7A and S7B show all vertical and horizontal shift factors from the TTS procedure vs. temperature for all valences.

The vertical shift factor accounts for slight changes in connectivity (Fig. S2) that result in an $\approx 40 - 80\%$ increase in G' (Fig. S7B). The horizontal shift factor accounts for changes in DNAns binding dynamics and exhibits an Arrhenius temperature-dependence (see section S2b, Fig. S8).

S2b. Relaxation times and Arrhenius dependence of relaxation times. The horizontal shift factor is the ratio between the DNAns network relaxation times at two different temperatures. For all f and [DNAns], the relaxation times show an Arrhenius temperature behavior, $\tau_c \propto \exp(E_A/RT)$ (Fig. S8), with an activation energy, E_a, that is independent of [DNAns] and f. Averaged over all [DNAns] and valences, $\langle E_a \rangle = 210 \pm 10$ kJ/mol.

This value is consistent with the enthalpy of binding of the overhang, $|\Delta H| = 239$ kJ/mol, which was calculated using the two-state melting application on the DINAmelt web server for overhang concentrations between 600μM and 3600μM at $T = 20$°C and 150mM NaCl (4, 5). Thus, for all f and [DNAns], the relaxation time τ_c of the network is determined by the kinetics of a single DNAns-DNAns bond.

S2c. Numerical estimate of solvent-drag-induced crossover frequency ('non-affine-to-affine model'). It has been shown that a Maxwellian crossover in G' and G'' can arise from solvent drag inducing a non-affine to affine transition in networks (6–8). Following ref. (6), a crossover induced by solvent drag should occur at a frequency $\omega_c \approx K_c/\alpha$, where K_c is the network chain's spring constant, and α is the drag coefficient of a node. We showed in the main text that $K_c \approx 10^{-4}$ N/m for a simple FJC model of DNAns arms; this was validated by the similarity of this value to estimated cluster spring constants. We then estimate the drag from a Stoke's picture: the drag of a sphere is $\alpha = 6\pi\eta a \approx 1.5 \times 10^{-10}$ N s/m, where $\eta \approx 1$ mPa s is the water viscosity, and the sphere radius $a \approx 8$ nm is set to the DNAns arm length. Note that this overestimates the drag, since the DNAns does not occupy all volume within the sphere, and leads to an underestimate of ω_c. Regardless, the crossover frequency is then $\omega_c \approx 7 \times 10^5$ Hz, which, while an underestimate, exceeds the measured crossover frequencies by five orders of magnitude. This indicates that the measured crossover is not caused by solvent drag, and supports the contention that it is instead caused by the kinetics of bond breakage (Section S2b).

S3. Strain sweep specific information

This section includes information regarding the strain sweep measurement, characteristic and yield strain measurements, and the uniaxial extension ratio calculation:

S3a. Linear and non-linear elasticity of DNAns networks. To investigate the linear and non-linear response of DNAns networks, we measured the storage, G', and loss, G'', modulus over a range of strains $1\% \leq \gamma \leq 200\%$ at a single frequency, $\omega > 62$ rad/s, and temperature, $T = 20°$C, using a discrete logarithmic sampling distribution of 10 points per decade. For all DNAns networks, G' and G'' were strain-independent for $\gamma \leq 10\%$, consistent with measuring a linear elastic response to applied deformation (Fig. S9). After the strain-independent regime, all networks, except for the two highest concentrated $f = 6$ networks, displayed resolvable strain hardening until yielding (Fig. S9). The hardening response of such networks are well fit by $G' \sim \exp\left((\gamma/\gamma^*)^2\right)$, where γ^* is the characteristic strain at which stiffening occurs (9–11) (see section S3b).

We observed that both the torque amplitude and radial displacement (*i.e.*, strain) amplitude time-trace were continuous at yielding (Fig. S10), consistent with rheometer plates maintaining contact to an elastic material. If the plate lost contact with the material at yielding, both traces would appear highly discontinuous and noisy.

S3b. Characteristic and yield strain. The non-linear elastic response of nearly all DNAns networks followed the relation $G'(\gamma) \sim \exp\left((\gamma/\gamma^*)^2\right)$, where γ^* is the characteristic strain at which strain hardening occurs. At a given f, γ^* remained either independent of or slightly increased with [DNAns] (Fig. S11A). On the other hand, as a function of f, γ^* decreased from $\approx 200\%$ at $f = 3$ to $\approx 110\%$ at $f = 6$ (Fig. S11A).

Given the digital nature of the non-linearity measurement, we defined the maximum strain, γ_m, as the strain at which $G'(\gamma)$ maximized. Moreover, we defined the error in maximum strain, γ_m, as the resolution of the data sampling. Note that a logarithmic sampling decreases in resolution as strain increases. Accordingly, we report larger errors for strains of greater values. Despite the large uncertainty in our measurement of γ_m, we observed that γ_m remained roughly independent of or slightly decreased with [DNAns] (Fig. S11B). As a function of f, γ_m decreased from $\approx 170\%$ at $f = 3$ to $\approx 20\%$ at $f = 6$ (Fig. S11B).

S3c. Uniaxial extension ratio calculation. The uniaxial extension ratio, $\lambda_{\max}$, of a polymer chain in a network is related to the characteristic strain of the network by (9):

$$\gamma^* = \lambda_{\max} - \lambda_{\max}^{-1} \qquad [6]$$

At a given f, $\lambda_{\max}$ remained roughly independent of or slightly increased with [DNAns] (Fig. S13). As a function of f, $\lambda_{\max}$ decreased as valence grew: for $f = 3, 4$, and 5, $\lambda_{\max} = 2.3 \pm 0.1, 1.7 \pm 0.1$, and 1.9 ± 0.2, respectively (Fig. S13). For the lowest concentrated $f = 6$ DNAns network, $\lambda_{\max} = 1.7 \pm 0.2$.

Arm number	Strand	Sequence (5′ to 3′)	Extinction Coefficient (L/(mole*cm))
f = 3	1	CTACTATGGCGGGTGATAAAAACGGGAAGAGCATGCCCATCCACGATCG	484100
f = 3	2	GGATGGGCATGCTCTTCCCGAACTCAACTGCCTGGTGATACGACGATCG	458900
f = 3	3	CGTATCACCAGGCAGTTGAGAATTTATCACCCGCCATAGTAGACGATCG	480500
f = 4	1	same as f = 3 strand 1	484100
f = 4	2	same as f = 3 strand 2	458900
f = 4	3	CGTATCACCAGGCAGTTGAGAACATGCGAGGGTCCAATACCGACGATCG	483300
f = 4	4	CGGTATTGGACCCTCGCATGAATTTATCACCCGCCATAGTAGACGATCG	469000
f = 5	1	same as f = 4 strand 1	484100
f = 5	2	same as f = 4 strand 2	458900
f = 5	3	same as f = 4 strand 3	483300
f = 5	4	CGGTATTGGACCCTCGCATGAACCATGCTGGACTCAACTGACACGATCG	462500
f = 5	5	GTCAGTTGAGTCCAGCATGGAATTTATCACCCGCCATAGTAGACGATCG	479800
f = 6	1	same as f = 5 strand 1	484100
f = 6	2	same as f = 5 strand 2	458900
f = 6	3	same as f = 5 strand 3	483300
f = 6	4	same as f = 5 strand 4	462500
f = 6	5	GTCAGTTGAGTCCAGCATGGAACGCATCAGTTGCGGCGCCGCACGATCG	465500
f = 6	6	GCGGCGCCGCAACTGATGCGAATTTATCACCCGCCATAGTAGACGATCG	467200

Fig. S1. Table of sequences used for each DNAns design and their respective extinction coefficients (taken from the oligo specification sheets sent by manufacturer). Complementary portions are colored identically, the sticky-end is highlighted in blue, and unbound nucleotides are highlighted in red.

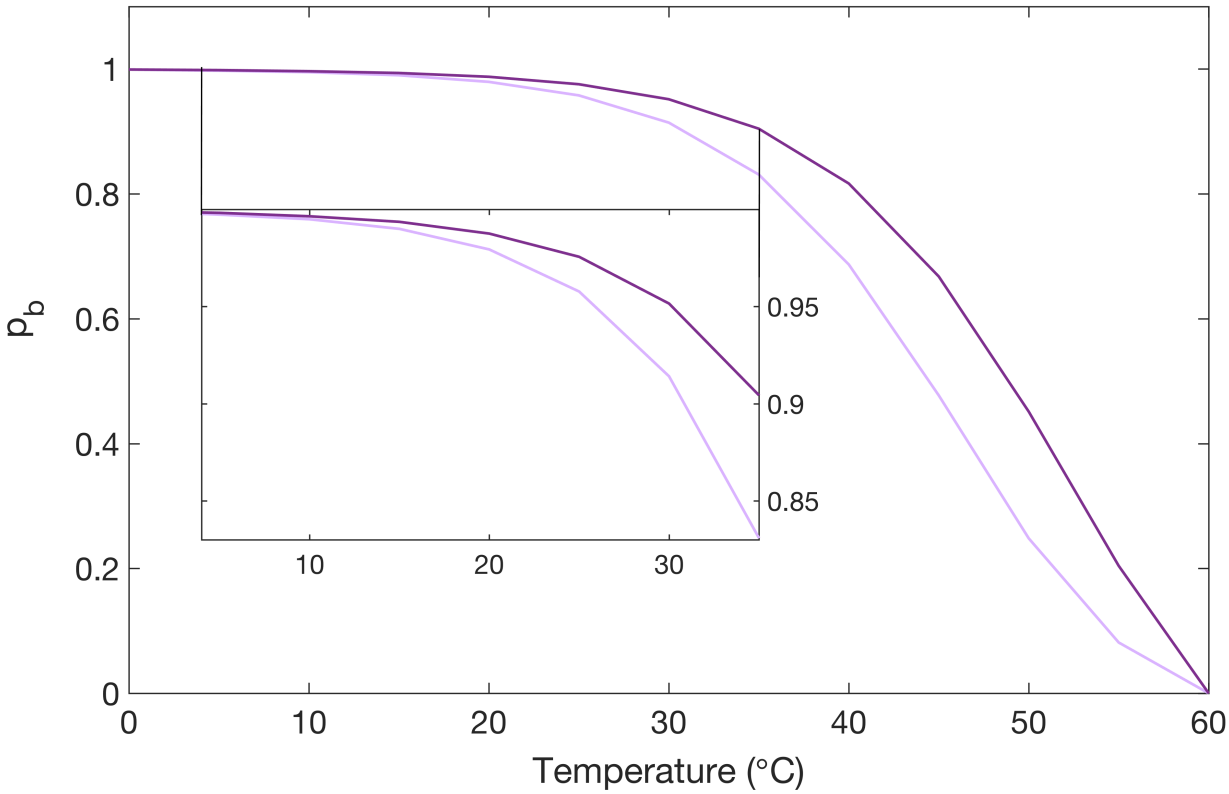

Fig. S2. Binding probability, p_b, of overhang sequence (5'-ACGATCG-3') duplex formation versus temperature at 150 mM NaCl. The light and dark purple line denote [DNAns] $= 600\ \mu$M$/f$ and [DNAns] $= 3600\ \mu$M$/f$, respectively. We note that the p_b reported is normalized to account for the two unbound A's in the DNAns-DNAns overhand bond, which were incorporated in the NUPACK calculation to account for their steric effects on duplex formation.

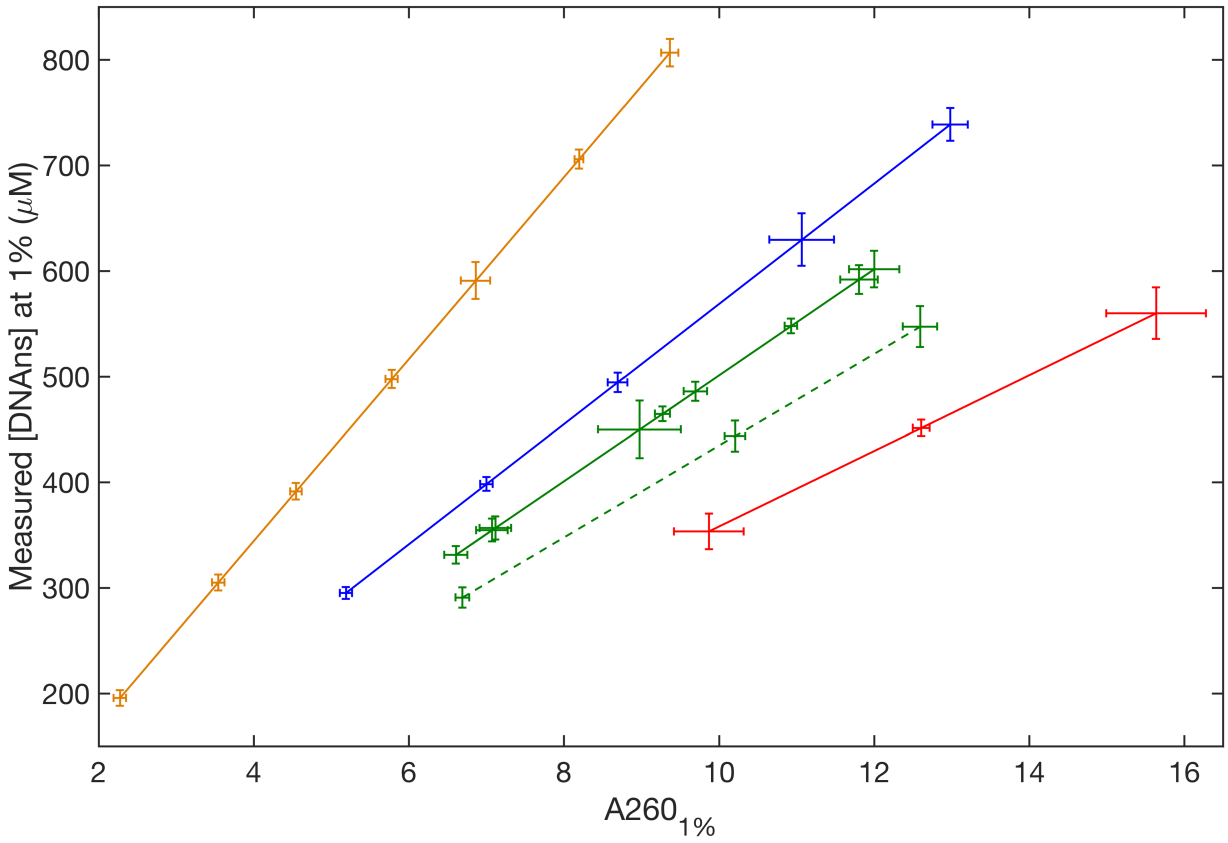

Fig. S3. Plot of measured [DNAns], with applied correction factors shown in Table S1, as a function of the measured A260 in the 1% dilutions, A260$_{1\%}$. The orange, blue, green, and red denote $f = 3, 4, 5,$ and 6, respectively. The lines are not fits, but an interpolated line connecting the data points meant as a guide for the eye. The dashed line denotes the second batch of $f = 5$ samples that was made several months after the first batch of $f = 5$ samples.

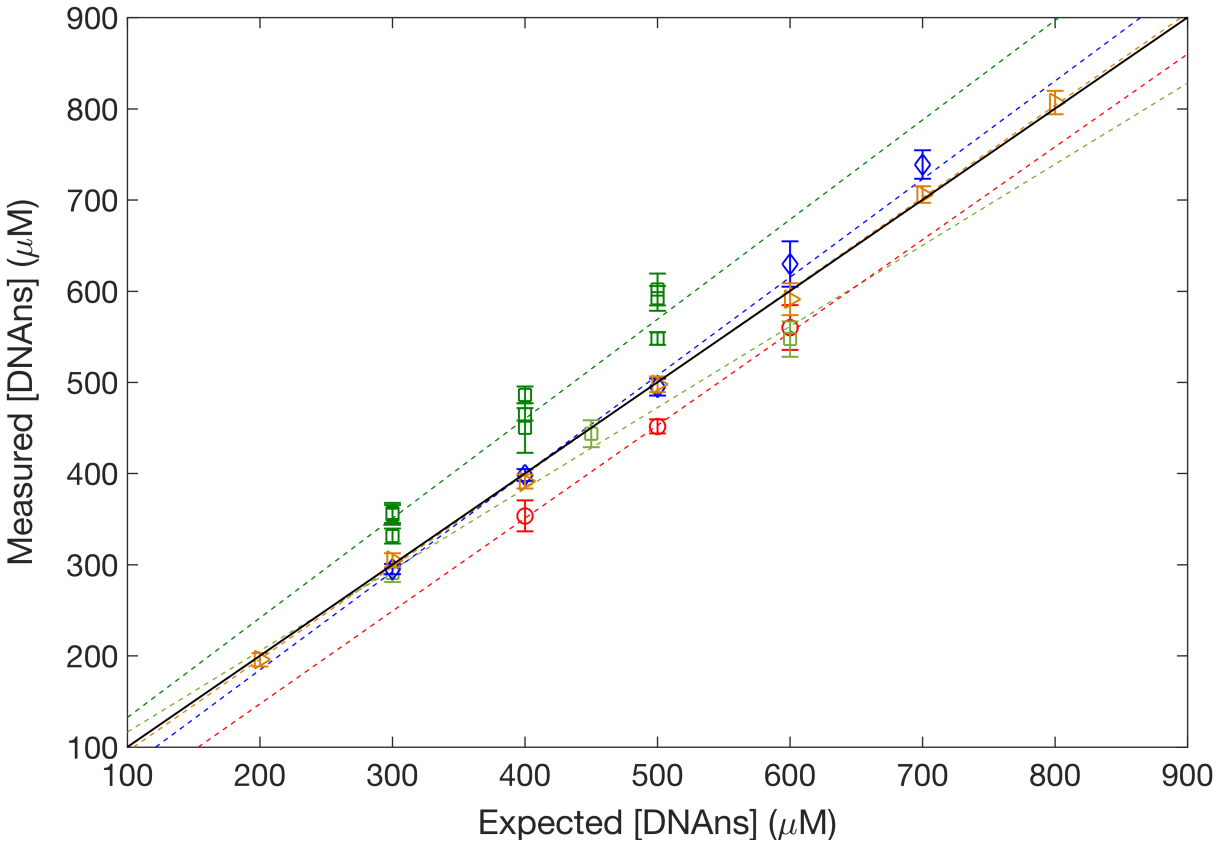

Fig. S4. Plot of measured [DNAns], with applied correction factors shown in Table S1, as a function of expected [DNAns]. The orange, blue, green, and red denote $f = 3, 4, 5$, and 6, respectively. The $f = 5$ samples colored in the lighter shade of green were made several months after the first batch of $f = 5$ samples (dark green) in order to reproduce mechanical measurements. The dashed lines denote linear fits to the data. The solid, black line denotes the relationship Measured [DNAns] = Expected [DNAns] (*i.e.*, $f(x) = x$).

f	A260$^*_{1\%}$	$100\cdot$A260$^*_{0.01\%}$	α	Correction to [DNAns]
3	9.4 ± 0.1	11.5 ± 0.3	$30 \pm 6\%$	1.23 ± 0.02
4	13.0 ± 0.2	14.0 ± 0.4	$72 \pm 7\%$	1.09 ± 0.02
5	7.1 ± 0.2	8.5 ± 0.5	$39 \pm 10\%$	1.19 ± 0.04
$^\times 5$	12.6 ± 0.1	13.0 ± 0.1	$89 \pm 20\%$	1.03 ± 0.05
6	15.6 ± 0.6	15.8 ± 0.3	$96 \pm 10\%$	1.01 ± 0.03

Table S1. Table of A260$^*_{1\%}$ and $100\cdot$A260$^*_{0.01\%}$ values as a function of f, along with the calculated percentage of ssDNA present at 1%, α, and the subsequent correction to [DNAns] at 1%. $^\times$This batch of $f = 5$ samples was made several months after the first batch of $f = 5$ samples in order to reproduce mechanical measurements.

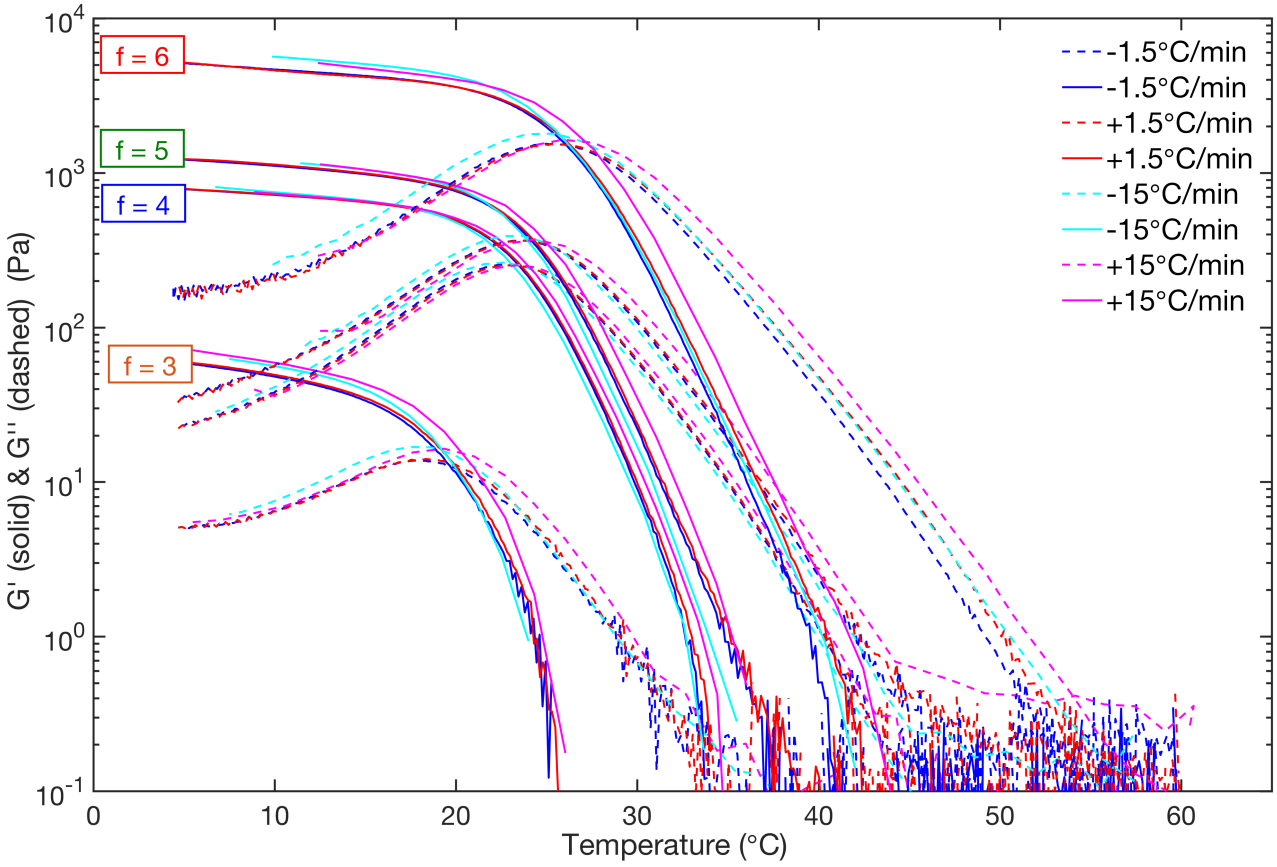

Fig. S5. Log-lin plot of G' and G'' vs. temperature at $\omega = 10$ rad/s and $\gamma = 5\%$ for different rates of cooling and heating (labeled in plot) of a (190 ± 10) μM 3-arm, (290 ± 10) μM 4-arm, (290 ± 10) μM 5-arm, and (360 ± 10) μM 6-arm DNAns solution. The overlap of the curves at different heating and cooling rates show that the viscoelastic response of the DNAns solution is independent of the rate of cooling and heating.

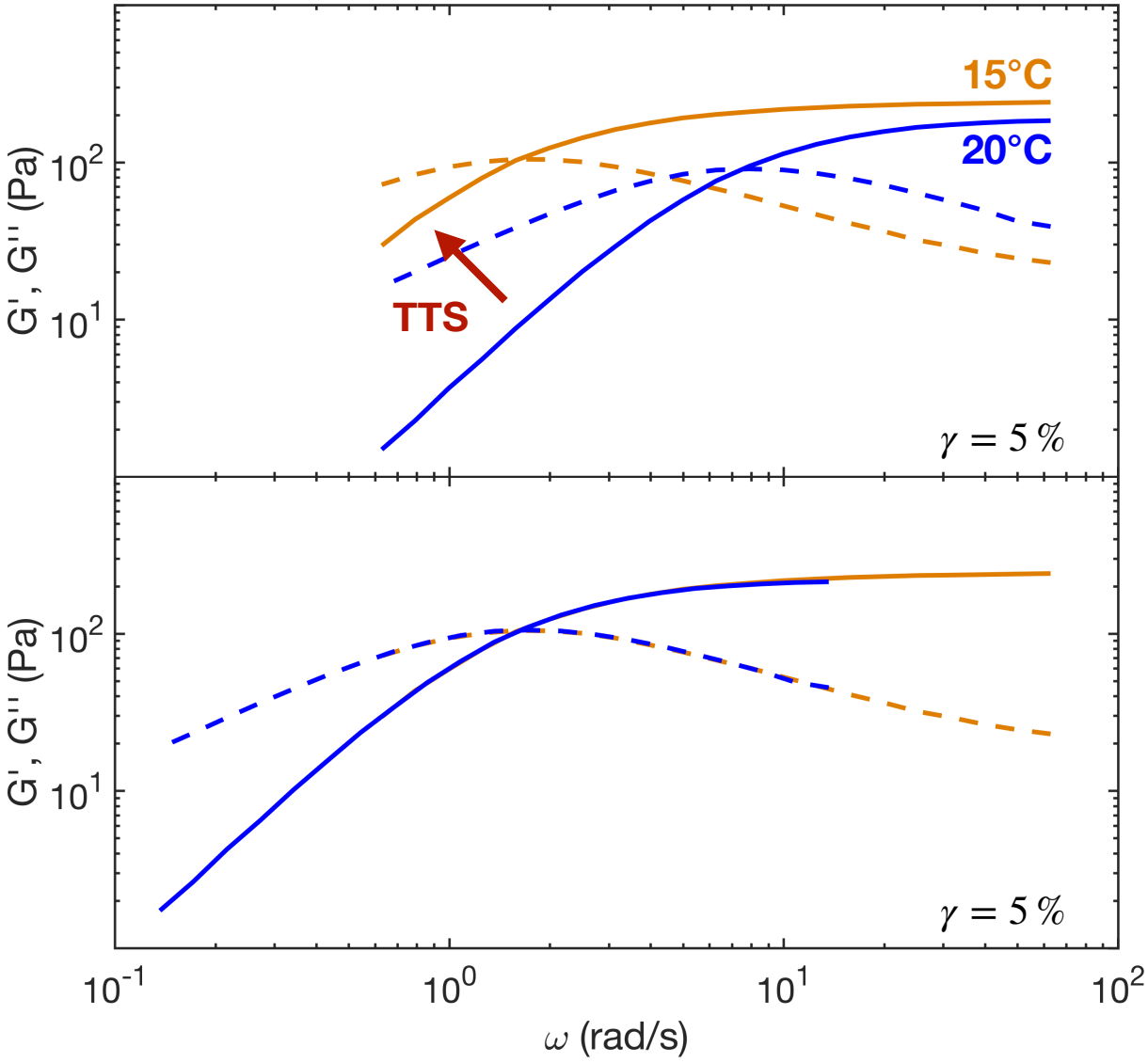

Fig. S6. The top and bottom panels are a log-log plot of $G'(\omega)$ and $G''(\omega)$ pre- and post-TTS, respectively. In this example, the reference temperature is $T_{\text{ref}} = 15°C$. As a note, the data shown is a subset of the $f = 3$ DNAns $G'(\omega)$ and $G''(\omega)$ data.

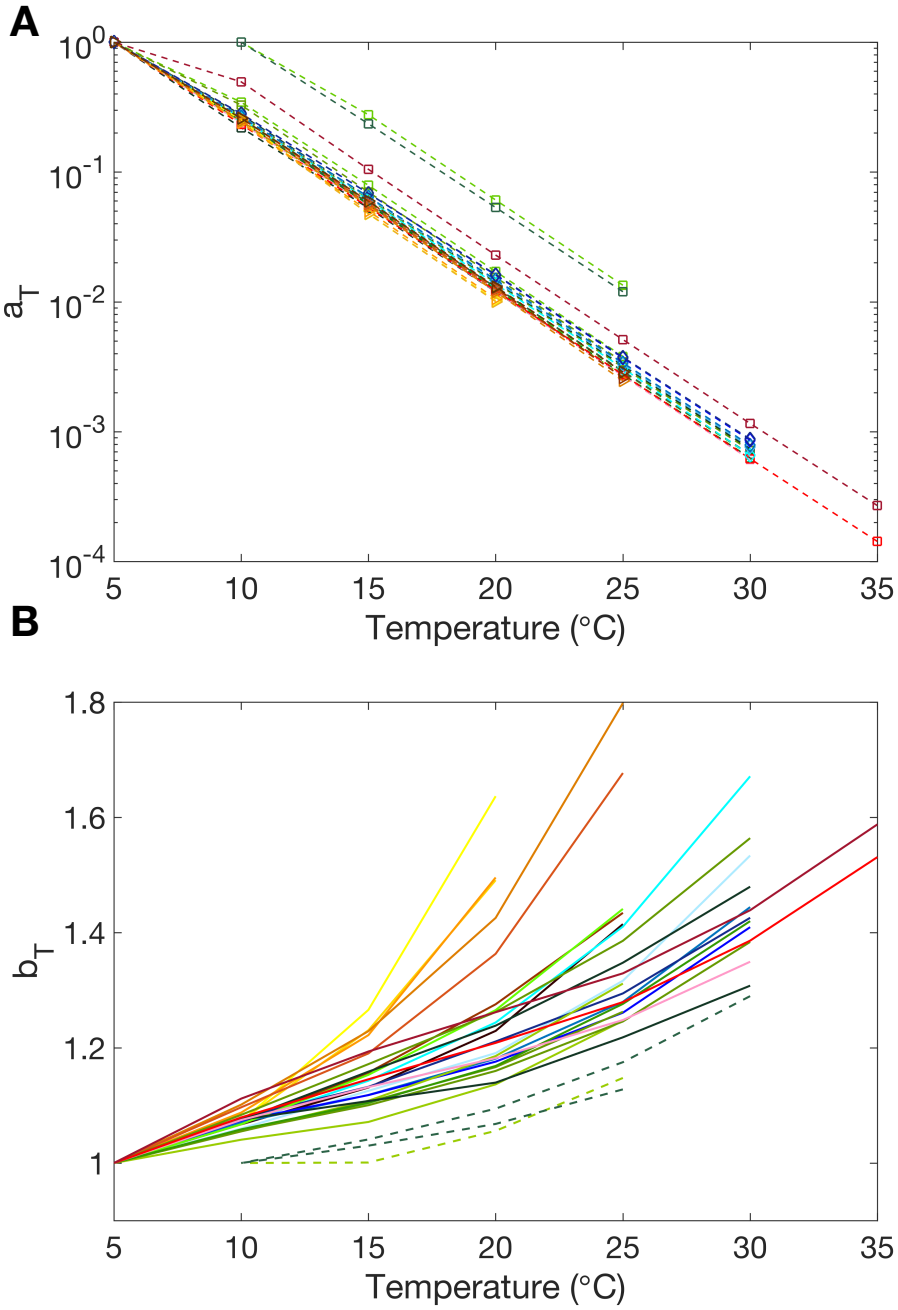

Fig. S7. Log-lin plot of the $T_{\text{ref}} = 5°\text{C}$ (A) horizontal shift factors, a_T, and (B) vertical shift factors, b_T, as a function of temperature. $f = 3, 4, 5$ and 6 are denoted by yellow triangles, blue diamonds, green squares, and red circles, respectively. The lines are guides for the eyes. The darker colored lines signify a higher [DNAns]. The dashed lines denote $f = 5$ samples that were not cooled to $T = 5°\text{C}$.

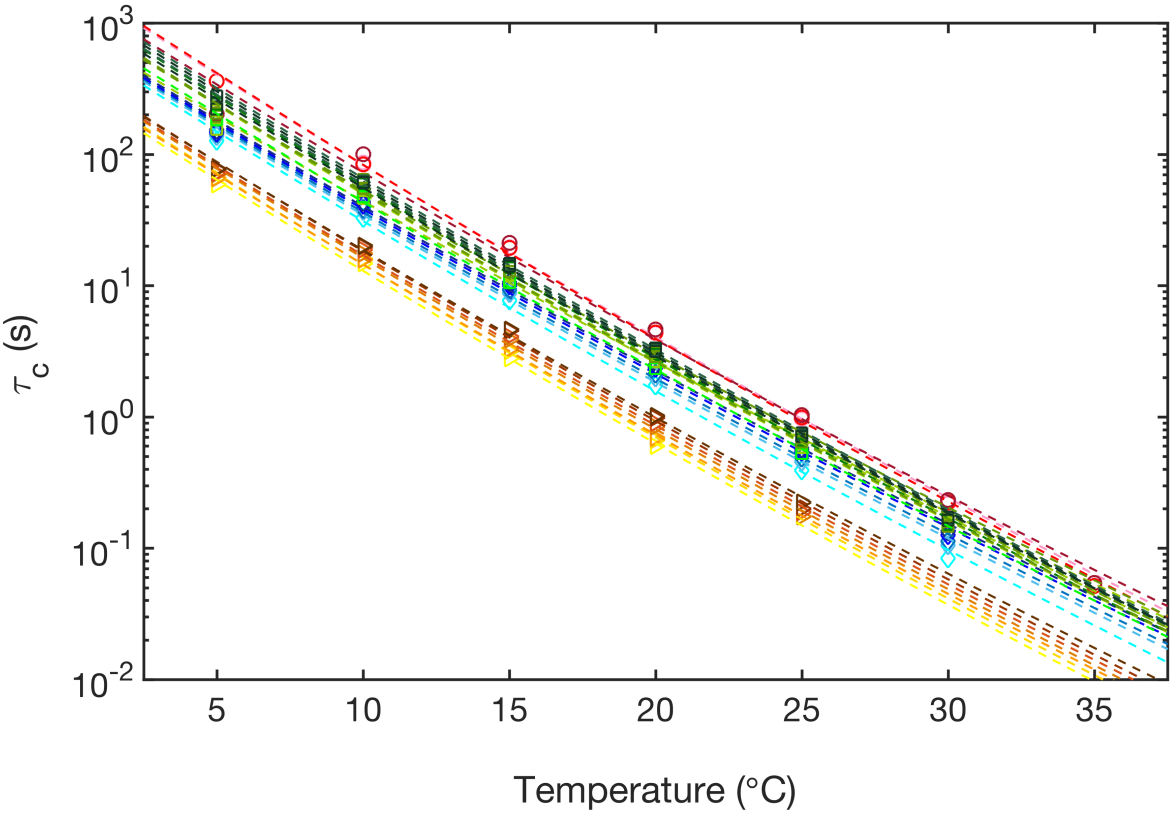

Fig. S8. Log-lin plot of the relaxation time, τ_c, as a function of temperature at $\gamma = 5\%$ for $f = 3$ (yellow triangles), 4 (blue diamonds), 5 (green squares), and 6 (red circles). Darker colors signify a higher [DNAns]. The dashed lines are the Arrhenius fits, $\tau_c \propto \exp(E_A/RT)$.

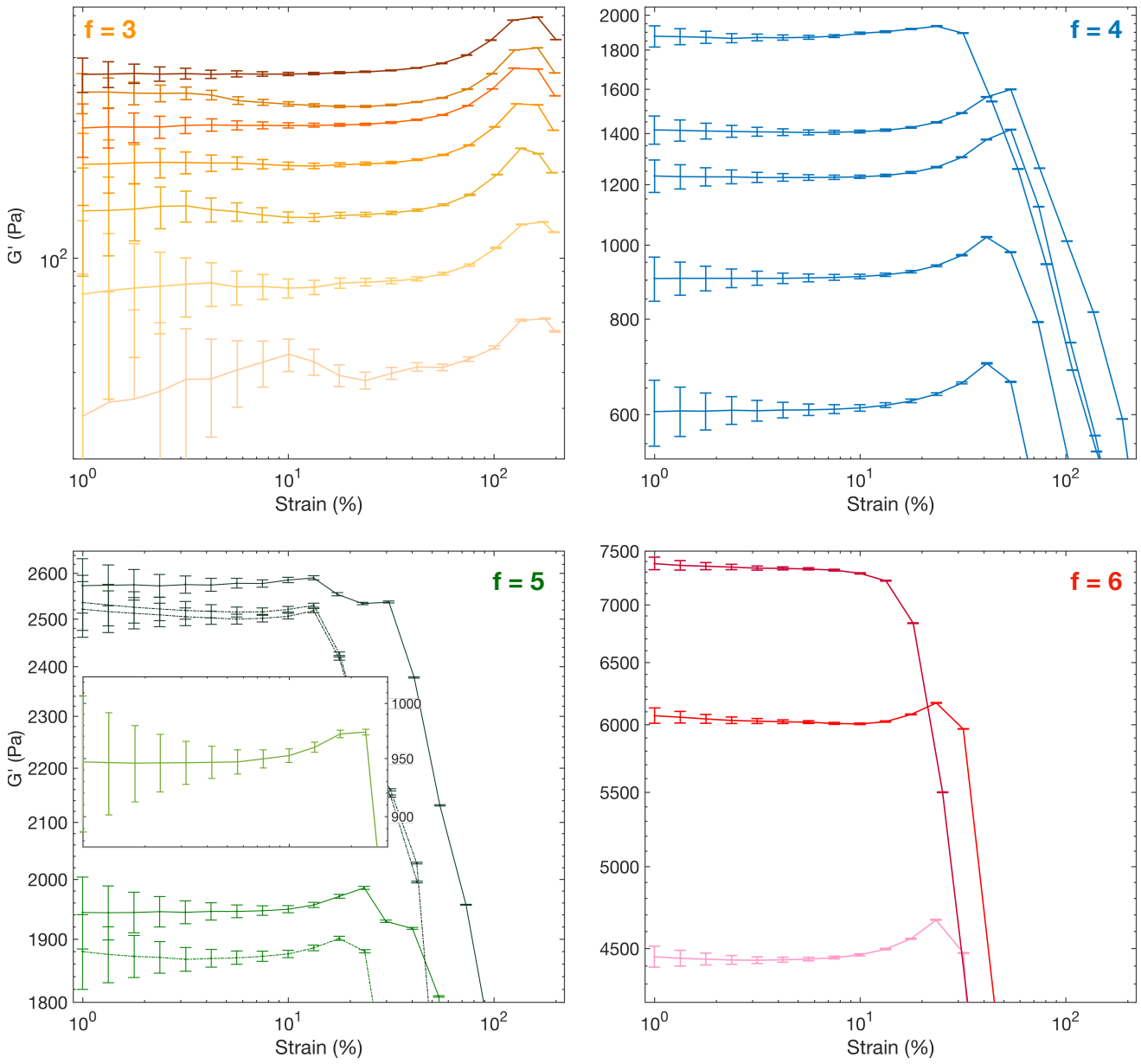

Fig. S9. Log-log plot of the storage modulus, G', as a function of strain, γ, at a temperature of $T = 20°C$ for $f = 3$ (top left panel), 4 (top right panel), 5 (bottom left panel), and 6 (bottom right panel). The curves with darker colors signify a higher [DNAns]. The solid and dash-dot lines denote data taken at a frequency of $\omega = 62.8$ rad/s and $\omega = 125.6$ rad/s, respectively. The inset of the $f = 5$ panel is the lowest concentrated $f = 5$ DNAns network, with $G' \approx 950$ Pa in the linear regime (scale on right of inset).

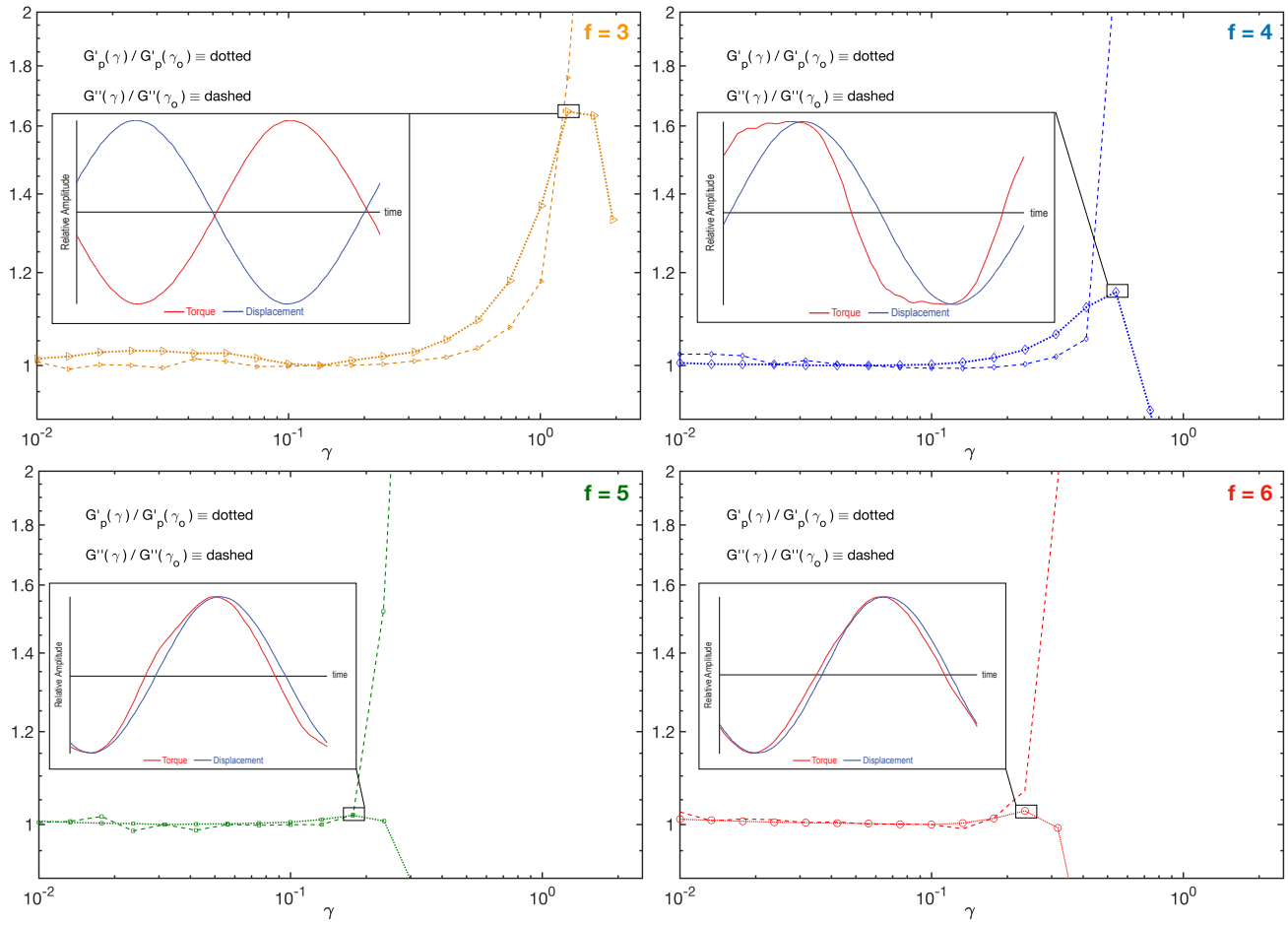

Fig. S10. Log-log plot of the normalized storage, $G'(\gamma)/G'(\gamma_o)$, and loss modulus, $G''(\gamma)/G''(\gamma_o)$ as a function of strain, γ, at a temperature of $T = 20°C$ of $f = 3$ at [DNAns] ≈ 500 μM (top left panel), $f = 4$ at [DNAns] ≈ 500 μM (top right panel), the $f = 5$ gel at [DNAns] ≈ 450 μM (bottom left panel), and $f = 6$ gel [DNAns] ≈ 450 μM (bottom right panel). The insets of each panel show the measured relative amplitude of the torque (red) and radial displacement (blue) wave-forms as a function of time at the point of yielding.

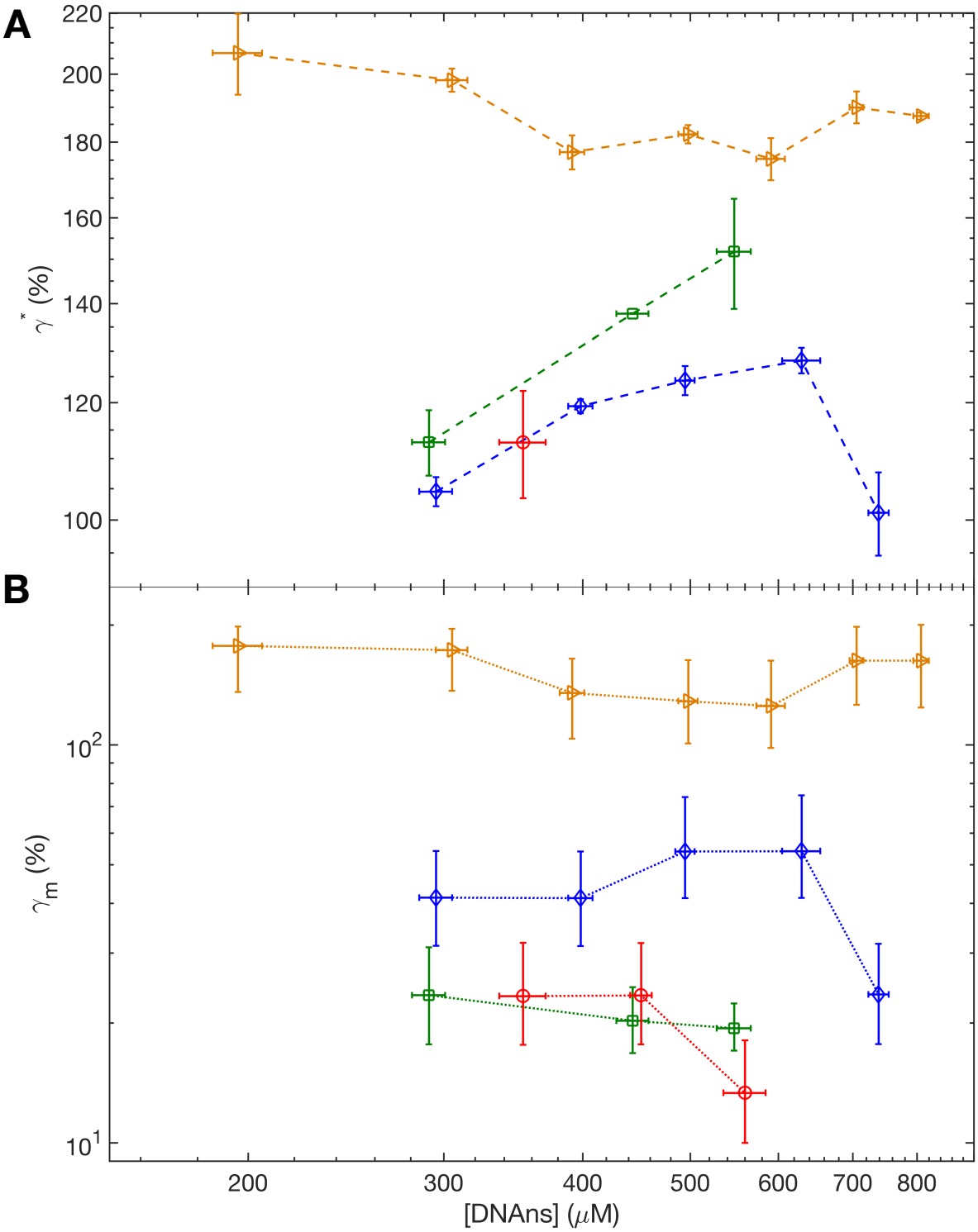

Fig. S11. **(A)** Log-log plot of γ^*, as a function of [DNAns] for f =3 (yellow triangles), 4 (blue diamonds), 5 (green squares), and 6 (red circles) at $T = 20°C$ and $\omega \geq 62.8$ rad/s. **(B)** Log-log plot of γ_m, as a function of [DNAns] for $f = 3$ (yellow triangles), 4 (blue diamonds), 5 (green squares), and 6 (red circles) at $T = 20°C$ and $\omega \geq 62.8$ rad/s. In **(A)** and **(B)**, the dashed and dotted lines are guides for the eye.

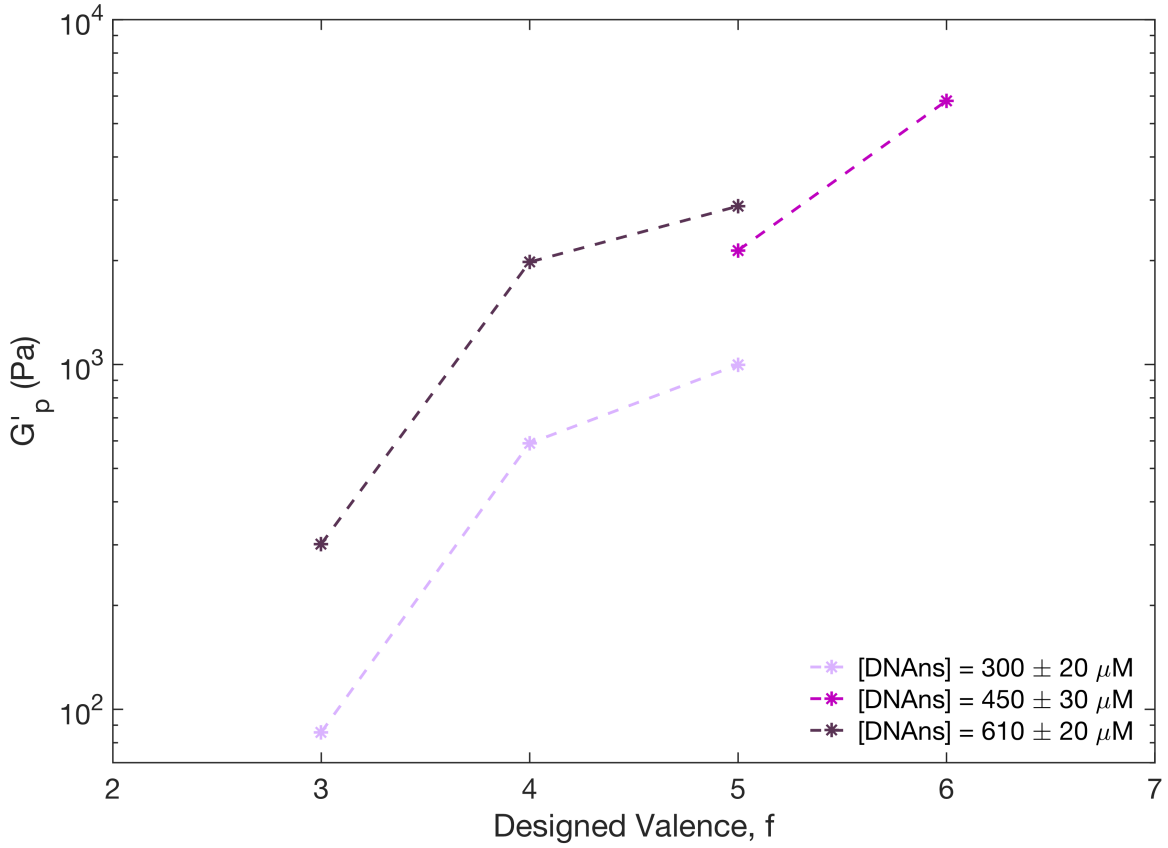

Fig. S12. Log-lin plot of the plateau modulus, G_p', as a function of designed valence, f, at $T = 20°$C and $\gamma = 5\%$. The DNAns concentration of each data set is given in the legend.

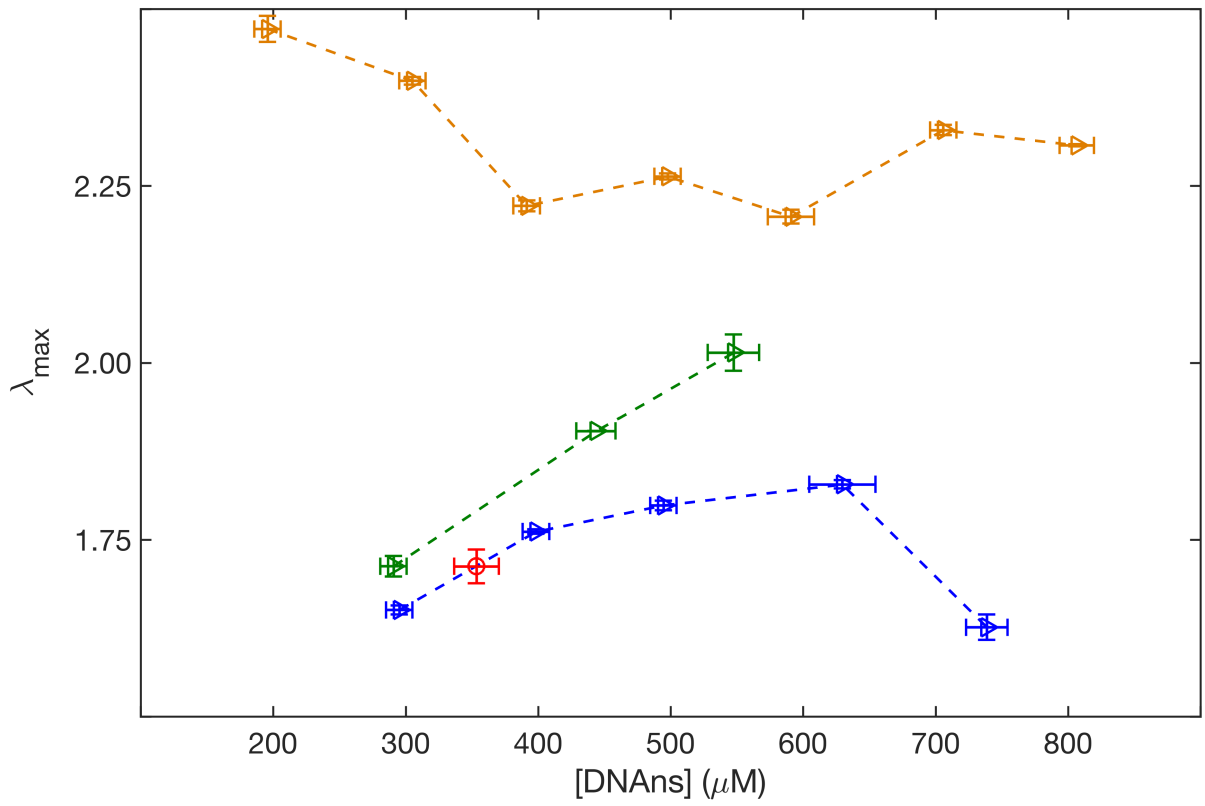

Fig. S13. Plot of $\lambda_{\max}$, as a function of [DNAns] for $f = 3$ (yellow triangles), 4 (blue diamonds), 5 (green squares), and 6 (red circles) at $T = 20°$C. The dashed lines are guides for the eye.

f	[DNAns] (μM)	ϕ_{rods}	ϕ_{sphere}	G'_p (Pa)
3	195	0.009	0.30	39.5
	305	0.015	0.47	85.6
	390	0.019	0.61	127
	500	0.024	0.77	215
	590	0.029	0.92	301
	705	0.034	1.09	388
	810	0.039	1.25	492
4	295	0.019	0.46	590
	400	0.026	0.62	915
	495	0.032	0.77	1240
	630	0.041	0.98	1460
	740	0.048	1.14	1980
5	290	0.023	0.45	996
	330	0.027	0.51	1370
	355	0.029	0.55	1380
	355	0.029	0.55	1400
	445	0.036	0.69	1940
	450	0.036	0.70	2140
	465	0.037	0.72	2185
	485	0.039	0.75	2140
	550	0.044	0.85	2630
	550	0.044	0.85	2800
	590	0.048	0.91	2820
	600	0.048	0.92	2870
6	350	0.034	0.55	4620
	450	0.044	0.70	5810
	560	0.054	0.87	7450

Table S2. Correspondence between [DNAns], DNAns volume fraction ϕ, and G'_p. ϕ is calculated in two ways: (i) ϕ_{rods} assumes the DNAns is composed of f rods, with each rod having a length given by the dsDNA arm length (8.5 nm, which includes half the sticky end) and radius (1 nm); and (ii) ϕ_{sphere} gives the volume fraction of a monodisperse system of spheres of concentration [DNAns], with the sphere radius set to the DNAns arm length (8.5 nm). ϕ_{sphere} is useful in gaining intuition on system structure through comparision to volume fractions of, *e.g.*, FCC or random-sphere packings (12, 13).

References

1. Zadeh JN, et al. (2011) Nupack: analysis and design of nucleic acid systems. *Journal of Computational Chemistry* 32(1):170–173.
2. Rovigatti L, Bomboi F, Sciortino F (2014) Accurate phase diagram of tetravalent dna nanostars. *The Journal of Chemical Physics* 140(15):154903.
3. Nwokeoji AO, Kilby PM, Portwood DE, Dickman MJ (2017) Accurate quantification of nucleic acids using hypochromicity measurements in conjunction with uv spectrophotometry. *Analytical Chemistry* 89(13567):13567–13574.
4. Markham NR, Zuker M (2005) Dinamelt web server for nucleic acid melting prediction. *Nucleic Acids Research* 33(Web Server Issue):W577–W581.
5. Markham NR, Zuker M (2008) *"UNAFold: software for nucleic acid folding and hybridization" in Bioinformatics, Volume II Structure, Function and Applications.* (Humana Press, New Jersey).
6. Yucht MG, Sheinmanb M, Broedersz CP (2013) Dynamical behavior of disordered spring networks. *Soft Matter* 9(7000):7000–7006.
7. Zhang L, Mao X (2016) Finite-temperature mechanical instability in disordered lattices. *Physical Review E* 93(022110):1–8.
8. Rocklin DZ, Hsiao LC, Szakasits M, Solomon MJ, Mao X (2018) Elasticity of colloidal gels: structural heterogeneity, floppy modes, and rigidity. *arXiv* 1808.01533v1:1–7.
9. Seitz ME, et al. (2008) Fracture and large strain behavior of self-assembled triblock copolymer gels. *Soft Matter* 5(2):447–456.
10. Erk KA, Henderson KJ, Shull KR (2010) Strain stiffening in sythentic and biopolymer networks. *Biomacromolecules* 11(5):1358–1363.
11. Douglas JF (2009) Elasticity of networks with permanent and thermoreversible cross-links. *MRS Proceedings* 1234:1234–QQ04–01.
12. Liu W, Jin Y, Chen S, Maksec HA, Li S (2018) Equation of state for random sphere packings with arbitrary adhesion and friction. *Soft Matter* 13(421):421–427.
13. Ziff RM, Torquato S (2017) Percolation of disordered jammed sphere packings. *Journal of Physics A: Mathematical and General* 50(8):1–12.